Published in final edited form as:

Biol Psychiatry Cogn Neurosci Neuroimaging. 2019 December ; 4(12): 1059–1069. doi:10.1016/j.bpsc.2019.06.013.

In trauma-exposed individuals, self-reported hyperarousal as well as sleep architecture predict resting-state functional connectivity in frontocortical and paralimbic regions

Jeehye Seo[a,b,c], **Katelyn I. Oliver**[a,b,c], **Carolina Daffre**[a,b,c], **Kylie N. Moore**[a,b,c], **Natasha B. Lasko**[a,b,c], **Edward F. Pace-Schott**[a,b,c]

[a]Massachusetts General Hospital, Department of Psychiatry, Charlestown MA, USA

[b]Harvard Medical School, Department of Psychiatry, Charlestown, MA, USA

[c]Athinoula A. Martinos Center for Biomedical Imaging, Charlestown, MA, USA

Abstract

Background: Symptoms of post-traumatic stress disorder (PTSD) reflect abnormalities in large-scale brain networks. In recently trauma-exposed individuals, we examined associations of seed-based resting-state functional connectivity (rsFC) with posttraumatic symptoms and sleep. We hypothesized that more severe PTSD symptoms and poorer sleep quality would predict (1) greater rsFC between fear-related seeds and other fear-related regions, and (2) lesser rsFC between fear-related seeds and emotion-regulatory regions.

Methods: Seventy-four participants who had experienced a DSM-5 Criterion-A stressor within the past 2 years varied from asymptomatic to fully meeting criteria for PTSD. They underwent 14 days of actigraphy and sleep diaries, a night of ambulatory polysomnography, and one fMRI resting-state scan at 3T. rsFC measures of five fear-related and one emotion-regulatory seeds with regions of the anterior cerebrum were correlated with PTSD symptomatology, objective and subjective habitual sleep quality and sleep architecture.

Results: Longer objective habitual sleep onset latency (SOL) was associated with greater connectivity between fear-related seeds and other regions of the salience network. Greater PTSD symptomatology was associated with less connectivity between fear-related seeds and anterior emotion-regulatory regions, while greater percent slow wave sleep (SWS%) was associated with more connectivity between these regions. However, other objective and subjective measures reflecting better habitual sleep quality were associated with lesser rsFC between these regions.

Conclusions: Longer SOL predicted greater rsFC among fear-related areas. More severe PTSD symptoms predicted lesser rsFC between fear and fear-regulatory regions reflecting putatively

Corresponding Author: Edward F. Pace-Schott, Ph.D., Harvard Medical School, Massachusetts General Hospital - East, CNY 149 13th Street, Room 2605, Charlestown, MA 02129, USA, Phone: 508-523-4288, Fax: 617-726-4078, epace-schott@mgh.harvard.edu.

reduced top-down fear regulation. Some (e.g., SWS%), but not all, sleep indices predicted greater top-down fear regulation.

Keywords

Trauma; PTSD; resting state functional connectivity; hyperarousal; salience network; emotion regulation

Introduction

Sleep disturbances such as insomnia and nightmares are ubiquitous and debilitating symptoms of posttraumatic stress disorder (PTSD) and are associated with substance abuse, depressive symptoms and suicidal ideation (1–4). PTSD is associated with increased threat sensitivity and fear generalization as well as deficits in attentional control and fear extinction (5–14). Such functions are controlled by anterior forebrain circuits involving the amygdala, insula, prefrontal cortex, and hippocampus (8, 15) and have been shown to be sensitive to sleep disruption (16–19). It is increasingly understood that psychiatric disorders like PTSD are disorders of specific neural pathways (15, 20, 21). An effective way to understand network connectivity, resting-state functional connectivity (rsFC), is an imaging method that exploits low frequency oscillations (0.008–0.1 Hz) of the blood oxygen level dependent (BOLD) fMRI signal during resting wakefulness. It is used to investigate relationships between large-scale intrinsic spontaneous brain activity in different regions (22–25), and has successfully defined at least seven widely distributed, stable brain networks (26–28). These seven networks include the default mode network (DMN), the salience network (SN), a central executive network (CEN), a dorsal attention network and, three networks corresponding to processing in the major sensory modalities (28–31).

Studies using rsFC have identified brain regions with altered activity and connectivity in individuals with PTSD compared to healthy subjects with and without previous trauma exposure. For example, using a region of interest (ROI) approach, Nicholson et al. (2016) showed differences between individuals with PTSD and dissociative symptoms, individuals with PTSD without such symptoms, and healthy controls in rsFC between insular sub-regions and the basolateral amygdala (32). Olson et al. (2018) examined rsFC between dorsolateral prefrontal (dlPFC) and anterior and posterior DMN seeds in persons with PTSD, trauma-exposed non-PTSD controls (TENC), and non-exposed controls, finding greater anti-correlation between dlPFC and posterior DMN (precuneus) in those with PTSD compared with other groups (33). When comparing an amygdala seed in a small sample of male veterans with PTSD to combat-exposed controls (34), veterans with PTSD showed greater amygdala-insular and lesser amygdala-hippocampal rsFC. In a qualitative review of 9 seed-based studies, Koch et al. (2016) reported greater rsFC within the salience network and lesser rsFC within the DMN in PTSD compared to controls (35).

The current study adopts the Research Domain Criterion (RDoC) approach (20, 36, 37) whereby a specific population is examined dimensionally across a range of both normal and abnormal values of specific symptoms. In this case, recently trauma-exposed adults are examined across a range of sleep quality and PTSD-symptom variables. Additionally, rather

than specify individual target ROIs in addition to seed ROIs, we examined rsFC between 6 symptom-relevant seeds and the entire anterior cerebrum. Five fear-related seeds were areas of the salience network believed important in fear expression while the sixth, the ventromedial prefrontal cortex (vmPFC), is a portion of the anterior DMN believed to exert top-down inhibition of fear (14). Although studies comparing resting neuronal activity levels between PTSD and controls have identified differences in posterior regions (35, 38, 39), seed-based rsFC studies have focused on anterior regions (see above). Moreover, major elements of emotion generation and emotional regulatory networks as well as key nodes of fear-expression and fear-extinction networks that are known to display task-based abnormalities in PTSD are all anteriorly localized (8, 14, 40, 41). Higher-level, cognitively based emotion regulatory structures, such as the lateral prefrontal cortices (42), may exert control over subcortical generators by recruiting midline limbic cortices such as the vmPFC (43).

We thus formed 2 hypotheses. Hypothesis 1 suggested that greater PTSD symptomatology and poorer sleep quality (including nightmares) would predict greater rsFC among fear-related seeds and other regions of the salience network. Hypothesis 2 suggested that greater PTSD symptomatology and poorer sleep quality would predict lesser rsFC between fear-related seeds and prefrontal regions related to cognitive control (CEN) and emotion regulation in lateral and medial prefrontal areas, the latter including the vmPFC and dorsomedial PFC (dmPFC). A corollary of Hypothesis 2 is that less PTSD symptomatology and better sleep quality would also predict greater rsFC between the vmPFC seed and CEN/mPFC areas, indicating a putatively greater coordination among areas subserving emotional and cognitive control.

Methods

Participants

Seventy-four, right-handed participants ranging from 18 to 40 years of age (mean = 23.5, SD = 4.5 (see Table 1) were recruited from the Boston metropolitan area using online and posted advertisements. All participants had experienced a DSM-5 criterion-A traumatic event (“index trauma”) in the past two years. Potential participants first completed a telephone screening and, if qualified, completed psychiatric and sleep interviews. Current and lifetime history of DSM-IV-TR Axis I psychiatric disorders were evaluated using the Structured Clinical Interview for DSM-IV for Non-Patients (SCID 1/NP) (44) and PTSD symptoms were assessed using the Clinician-Administered PTSD Scale for DSM-5 (CAPS-5) (45) and the PTSD Checklist for DSM-5 (PCL-5) (46). See Supplementary Materials for descriptions of the sleep disorder evaluation and exclusion criteria. All study procedures were approved by the Partners Healthcare Institutional Review Board. All participants provided written informed consent and were paid for their participation.

Psychopathology Severity Indices

The PCL-5 was used to measure overall PTSD severity. A composite hyperarousal index (CHI) was calculated from the hyperarousal (Cluster E) items from the CAPS and PCL-5 by

first converting each assessment's hyperarousal-item totals to a 0–100 scale and then averaging these 2 scores. (see Table 1 and Supplementary Methods).

Habitual sleep monitoring period and questionnaires

Participants underwent an approximately 2-week (mean 14.6± 2.9 nights) sleep-assessment period with wrist actigraphy and sleep diaries that also contained a nightmare questionnaire. Following an acclimation/sleep-disorders diagnostic night using ambulatory polysomnography (PSG), ambulatory PSG was repeated on the night before their resting state fMRI scan. No participants were excluded for obstructive sleep apnea (OSA) or periodic limb movement (PLMS) sufficient to warrant referral for treatment. Additionally, participants were prohibited from consuming alcohol or recreational drugs throughout this period and instructed to not consume caffeine or take daytime naps the day before or the day of their scan. During the sleep-monitoring period, participants completed an online battery of questionnaires (see Table 1).

Actigraphy and sleep diaries

During the 2-week sleep-assessment period, participants continuously wore the Actiwatch-2 (Phillips Respironics, Bend, OR) and pressed an event-marker before attempting to sleep in the evenings and when they first woke up in the morning. Event-markers were used to time stamp the time-in-bed (TIB). Within this period, the default algorithm of Actiware 5.61 software determined total sleep time (TST), sleep onset latency (SOL), and sleep efficiency (SE: total sleep time in minutes divided by TIB; Table 1). Actiwatch SOL and SE estimates have been validated with in-lab PSG and are considered good estimates of these measures (47, 48). When button-presses were missed, times recorded on diaries were substituted, which occurred 18.9% of the time. If both button-presses and diary records were missing for a particular night, that night was excluded from the final analysis. Actiwatch data for 5 subjects were excluded due to malfunction (N=69).

The Evening-Morning Sleep Questionnaire diary (EMSQ) (49, 50) provided subjective TST, SOL, and SE during the sleep-monitoring period (Table 1; see Supplementary Methods for computation details). EMSQ data for 4 subjects were omitted due to incomplete diaries (N=70).

Dream reports

Upon waking, 69 participants completed a dream questionnaire asking whether a dream was recalled, whether it was a nightmare (causing awakening) or a bad dream, and the degree to which it resembled their trauma (exactly, similar, possibly similar, or unrelated). Per-total-diary percentages for nightmares, bad dreams, the sum of bad dreams and nightmares, as well as the sum of dreams that were exactly-like/similar to the trauma were calculated as nights with specific dream types divided by total nights studied.

Ambulatory PSG

The Somte-PSG monitor (Compumedics USA, Charlotte, NC) was used with a standard montage (see Supplementary Methods for details). Sleep stage percentages, sleep onset

latency (SOL), REM latency and sleep efficiency (SE %) were computed from scored records. Due to artifact in recordings, 13 subjects were excluded from final analyses (N=61).

MRI Image Acquisition

Whole brain images were collected with a 3 Tesla Siemens MAGNETOM Prisma scanner (Siemens Medical Systems, Iselin, New Jersey) and a 32-channel head coil. First, automated scout images and shimming procedures were performed to optimize field homogeneity. High-resolution 3D T1 MEMPRAGE sequences (TR/TE1,2,3,4/flip angle=2530 ms/ 1.69,3.55,5.41,7.27 ms/7°) were collected with an in-plane resolution and slice thickness of 1.0 mm. Following these anatomical scans, 240 resting-state fMRI (rs-fMRI) blood oxygenation level dependent (BOLD) images were acquired with an interleaved T2*-weighted EPI sequence. Forty-six slices per TR were obtained with the following parameters: 2.5 mm slice thickness, 3×3 mm in-plane resolution, TR=2560 ms, TE=30 ms, flip angle=90°. Total scan time was 10 min and subjects were told to keep their eyes open and fixated on a white cross projected onto a screen.

rs-fMRI Data Analysis

MATLAB v2014a (The Mathworks Inc, Natick, Massachusetts, USA) and Statistical Parametric Mapping (SPM8; Wellcome Trust Centre for Neuroimaging, www.fil.ion.ucl.ac.uk) were used to process BOLD images and perform statistical analyses on rs-fMRI data. During pre-processing, functional images underwent slice timing, realignment, co-registration with the structural images, normalization into MNI space, and smoothing with an 8mm full width half-maximum Gaussian kernel to increase the signal-to-noise ratio and account for between-subject anatomical variations.

Resting-state functional connectivity analyses were performed using CONN functional connectivity toolbox v.17c (http://www.nitrc.org/projects/conn) (51). All imaging data were band-pass filtered (0.008 – 0.09 Hz) to reduce low-frequency drift and noise effects, and physiological and other spurious noise sources in the BOLD signal were removed using the anatomical component-based noise correction (CompCor) strategy implemented in CONN (52). White matter signals, cerebrospinal fluid signals, and six motion-correction parameters obtained from the pre-processing procedure were also removed.

Following pre-processing, maps of functional connectivity were obtained by plotting the correlation strength between the mean time course of a seed region to that of each voxel using the seed-to-voxel analysis. Key nodes in fear and extinction networks were selected as seed regions. Five fear-related regions were selected, including the left and right amygdala, left and right anterior insula cortex (AIC), and dorsal anterior cingulate cortex (dACC). Additionally, one fear-regulatory region in the ventromedial prefrontal cortex (vmPFC) (14, 53) was included for a total of six seed regions.

The amygdala and insular cortex seed regions were selected using parameters from the Automated Anatomical Labeling atlas (AAL, http://qnl.bu.edu/obart/explore/AAL/) (54) and using the WFU PickAtlas software interface (http://fmri.wfubmc.edu/software/PickAtlas) (55). The vmPFC and dACC seed coordinates were chosen based on a meta-analysis of 298 fear-related studies from the *NeuroSynth* database (www.neurosynth.org) (56) that have also

employed in previous seed-based rsFC studies (57). These seeds were defined by 6mm-diameter spheres with peak coordinates for the vmPFC at [6, 40, −20]; dACC at [0, 14, 28]; left AIC at [−32, 16, −10]; right AIC at [38, 16, −10]; left amygdala at [−24, −4, −18]; and right amygdala at [26, 0, −22]. Although the vmPFC axial coordinate is positive, indicating right-hemisphere laterality, the 6 mm sphere crosses the midline (axial coordinates from −1 to +9). Similarly, the 6 mm dACC sphere appears in both the left (–4) and right (+4) hemispheres.

The mean time series for each seed region was calculated and then correlated with the time courses of each voxel throughout the whole brain. The resulting coefficients were converted to normally distributed scores using Fisher's r-to-z transformation to give maps of voxel-wise functional connectivity for each seed region of interest (ROI) per participant. The value for each voxel represents its relative degree of functional connectivity to each seed (58). These maps were subsequently used for second-level analysis of relative functional connectivity using multiple regression analysis to investigate relationships of seed-to-voxel connectivity with psychopathology and sleep measures. To control for the potential effect of duration between trauma-exposure and the start of the study, time since trauma (Table 1) was entered as a covariate of no interest along with age and sex.

In second-level analyses, correlation maps were restricted to an anterior cerebral mask (see Figure S1 and its legend for specific regions). Although posterior regions might correlate meaningfully with sleep and hyperarousal variables, we chose this approach as a compromise between greatly restricting target ROIs (e.g., to only the seeds themselves) and whole-brain second-level analyses. Doing so, we increased statistical power by reducing the total number of voxels while continuing to examine the majority of putative emotion expression and regulatory regions. In order to rule out potentially meaningful correlations within posterior regions, we investigated seed-to-whole brain connectivity and performed additional analyses (see supplemental materials; Table S2).

Corrections for multiple comparisons were conducted with nonparametric permutation analyses (SnPM) using a toolbox for SPM (http://warwick.ac.uk/snpm; SnPM13) (59) using the following steps. The results of second-level analyses were first thresholded at cluster-defining threshold (CDT) $p<0.001$. A more rigorous analysis using SnPM was then performed to determine which clusters contained sufficient numbers of contiguous voxels that the likelihood of family-wise (Type-1) error (FWE) for that cluster was $p<0.1$ and $p<0.05$ following 5000 permutations. Such nonparametric permutation analysis is a highly conservative adjustment determined to be the most effective for controlling FWE by Eklund et al. (2016) (60). Mean z-scores of clusters showing significant correlation with psychopathology and sleep variables and surviving the SnPM FWE correction were extracted using the REX (Region of Interest Extraction) toolbox (http://web.mit.edu/swg/software.htm).

Outcome and predictor variables

To briefly reiterate, SPM8 first identified each voxel (within our anterior cerebral mask) whose connectivity (z-score) with a specific seed correlated with a specific predictor (e.g., PCL-5) at $p<0.001$. Such voxels, if contiguous, formed clusters of varying sizes (numbers of

voxels). SnPM13 then determined the minimum size that a cluster must be in order to be certain at $p<0.1$ (and usually $p<0.05$) that this cluster was not a false positive. In those clusters that survived SnPM correction for FWE, z-scores for each voxel were averaged. This mean z-score was the primary outcome variable whose association with the predictor variable was then tested using simple regression.

To reduce Type-1 error, a limited subset of variables predicting rsFC was chosen, *pre-hoc*, among the symptom and sleep measures (Table 1). These included PCL-5, CHI, actigraph and diary TST, SOL and SE, nightmares-plus-bad-dreams on a per-diary basis, as well as slow wave sleep percent (SWS%) and REM% from ambulatory PSG. The CHI was computed in order to assess PTSD hyperarousal symptoms separately from remaining PTSD symptoms (46). Actigraphy and sleep diaries captured objective and subjective habitual sleep quality respectively. Combining bad dreams and nightmares allowed a larger number of participants with non-zero values (59 vs. 35) although zero values remained included. From PSG, only SWS% and REM% were examined as these are the sleep stages from which the most prominent architectural anomalies are noted in the early post-trauma period as well as in diagnosed PTSD (16, 61, 62).

Statistical analyses

Analyses performed in SPM8 are described above. SPSS version 24 for Macintosh was used to perform simple regressions to examine the magnitude and direction of associations between predictor variables and mean z-scores extracted from clusters that survived SnPM FWE correction. In regressions, $p<0.05$ was considered statistically significant.

Results

Mean values and range of demographic, PTSD-symptom and sleep variables are shown in Table 1. Predictors chosen *pre-hoc* for correlation with rsFC are indicated.

Higher PCL-5 and CHI were each associated with less rsFC between right amygdala seed and right middle frontal cortex (MFC). Using SPSS, simple regression analysis showed that both the PCL-5 scores and CHI were negatively correlated with right amygdala seed to right MFC mean z-scores. No other regions associated with PTSD severity or CHI survived SnPM correction (Table 2 and S3, Figure 1).

Higher Actigraph TST was associated with less rsFC between (1) left amygdala seed and dmPFC, (2) vmPFC seed and right MFC, and (3) left amygdala seed and right MFC. In contrast, higher Actigraph TST was associated with greater rsFC between vmPFC seed and bilateral hippocampus. Simple regression showed that Actigraph TST was negatively correlated with (1) left amygdala seed to dmPFC, (2) vmPFC seed to right MFC, and (3) left amygdala seed to right MFC mean z-scores. Actigraph TST was positively associated with vmPFC seed to bilateral hippocampus mean z-scores. No other regions survived SnPM correction (Table 2 and S3, Figure 2).

Higher Actigraph SOL was associated with greater rsFC between (1) dACC seed and bilateral posterior insular cortex (PIC), (2) left amygdala seed and bilateral insular cortex

(IC), (3) vmPFC seed and right primary motor cortex (M1); and (4) left AIC seed and right MFC. Simple regression showed that Actigraph SOL was positively correlated with (1) dACC seed to right and left PIC, (2) left amygdala seed to bilateral IC, vmPFC seed to right M1, and (4) left AIC seed to right MFC mean z-scores. No other regions survived SnPM correction (Table 2 and S3, Figure S2).

Higher Actigraph SE was associated with less rsFC between vmPFC seed and supplementary motor area (SMA). Simple regression analyses showed that actigraph SE was negatively correlated with vmPFC seed to SMA mean z-scores. No other regions survived SnPM correction (Table 2 and S3, Figure S3).

Higher Diary TST was associated with less rsFC between left AIC seed and subgenual ACC (sgACC). In contrast, higher Diary TST was associated with greater rsFC between dACC seed and rACC. Simple regression analyses showed that Diary TST was negatively correlated with dACC seed to sgACC mean z-scores and positively associated with dACC seed to rACC mean z-scores. No other regions survived SnPM correction (Table 2 and S3, Figure S4).

Higher Diary SOL was associated with greater rsFC between right AIC seed and (1) pre-supplementary motor cortex (pre-SMA), and (2) left temporal pole. Simple regression analyses showed that SOL was positively correlated with (1) right AIC seed to pre-SMA, and (2) right AIC seed to right temporal pole mean z-scores. No other regions survived SnPM correction (Table 2 and S3, Figure S5).

A higher rate of combined nightmares and bad dreams was associated with less rsFC between left AIC seed and left orbitofrontal cortex (OFC) but greater rsFC between (1) dACC seed and rACC, (2) left amygdala seed and left M1, and (3) vmPFC seed and SMA. Simple regression analyses showed that nightmare and bad dream rates were negatively correlated with left AIC seed to left OFC mean z-scores, but positively correlated with (1) dACC seed to rACC, (2) left amygdala seed to left M1, and (3) vmPFC seed to SMA mean z-scores. No other regions survived SnPM correction (Table 2 and S3, Figure 3).

Higher PSG SWS% was associated with greater rsFC between right amygdala seed and (1) dmPFC, and (2) rACC. Simple regression analyses showed that SWS% was positively correlated with (1) right amygdala seed to dmPFC and (2) right amygdala seed to rACC mean z-scores. No other regions survived SnPM correction (Table 2 and S3, Figure 4).

Discussion

Greater actigraph SOL predicted greater connectivity between both the left amygdala and the dACC seeds with bilateral PIC. As all these areas fall within the salience network, these findings support Hypothesis 1.

Findings on PTSD symptomatology generally supported Hypothesis 2 with both greater hyperarousal (CHI) and greater levels of non-hyperarousal symptoms (PCL-5) predicting lesser rsFC between the right amygdala seed and right MFC. (Note that, after SnPM correction, both CHI and PCL-5 scores predicted this same rsFC finding at an FWE of $p<0.1$

but the PCL-5 score additionally predicted significance at $p<0.05$.). PSG sleep architecture findings also supported Hypothesis 2. Greater SWS% predicted greater connectivity between the right amygdala seed and the dmPFC and rACC. This latter finding is of particular interest as diminished SWS, relative to controls, was one of few consistent sleep abnormalities reported in a meta-analysis of sleep studies in PTSD (61). Notably, SWS has been recently linked with emotional processing (63, 64).

In the case of habitual sleep measures, however, results were divided between those supporting and failing to support Hypothesis 2. Greater diary TST predicted greater rsFC between the dACC seed and rACC, an emotion regulatory area (57, 65, 66) thus according with Hypothesis 2. Similarly, a greater rate of nightmares predicted lesser rsFC between the left AIC seed and the left OFC. However, contradicting Hypothesis 2, greater actigraph TST predicted lesser rsFC between the left amygdala seed and the dmPFC and right MFC as well as lesser rsFC between the vmPFC seed and the right MFC. Similarly, greater actigraph SOL predicted greater rsFC between the left AIC seed and right MFC. Moreover a greater rate of nightmares predicted lesser rsFC between the dACC seed and the rACC, and less diary TST predicted greater rsFC between the left AIC seed and the sgACC (BA25), an area that has been linked with fear extinction (67).

Several predictors were associated with rsFC between specific seeds and regions not clearly related to our 2 hypotheses including the hippocampus, M1, SMA, pre-SMA, and temporal pole. The hippocampus is believed to provide contextual information that disambiguates potentially fearful situations and, as such, some investigators assign it an emotion regulatory role (8, 14). If this is the case, then the fact that greater actigraph TST predicted increased rsFC between the vmPFC seed and bilateral hippocampi would support Hypotheses 2.

Greater nightmare/bad dream rate predicted greater rsFC between the left amygdala seed and left M1 Speculatively, this might represent greater readiness to react motorically to fear stimuli conveyed directly to the amygdala from the thalamus via the “low road” bypassing sensory and associative cortices (68). As such, this would support Hypothesis 1.

The SMA, and particularly the pre-SMA, are believed to be involved in motor control, particularly inhibition of ongoing motor sequences in service of initiating new behavior (69), possibly in response to detection of error or conflict (70). As such, these areas of the dmPFC may be considered to exert executive control. Thus, greater actigraph SE predicting lesser rsFC between the vmPFC seed and the SMA, greater nightmare rate predicting greater rsFC between the vmPFC seed and SMA and greater diary SOL predicting greater rsFC between the right AIC seed and pre-SMA would all appear to contradict Hypothesis 2. Nonetheless, other investigators have suggested the SMA/pre-SMA might be considered part of the salience network given their putative functions in initiating and switching behavior in response to salient stimuli (30, 71). From this viewpoint, the third (diary SOL) finding above would support Hypothesis 1.

Lastly, the temporal pole (BA38), although clearly an important limbic structure involved in socioemotional information processing (72), is not clearly involved in either the salience or

fear networks or in top-down control of emotion. hence its rsFC is difficult to interpret relative to Hypotheses 1 and 2.

There are a number of factors that limit the generalizability of these findings. First, although a comparatively large sample was analyzed, it was not as large as might ultimately be required to maximize confidence in these findings and we adopted an FWE threshold of $p<0.10$ so as to avoid Type 2 error. Second, seed-based rsFC restricts analyses to connectivity with specified seed regions and connectivity from adjacent regions having similar functional significance as these seeds is necessarily not sampled. A much larger sample, however, would be required to examine connectivity between every pair of voxels (31). Third, our sample is weighted toward young, female, educated, community-recruited individuals exposed to civilian trauma. Fourth, a 2-year window for an index trauma allows additional factors to intervene including incident co-morbidity and treatment. A sample obtained from a narrower window, although much more difficult to obtain, would provide greater confidence in the specific association of findings with the index trauma.

Conclusions

In recently trauma-exposed individuals spanning the range from asymptomatic to PTSD-diagnosed, longer average objective SOL was associated with greater connectivity between fear-related seeds and other regions of the salience network. Greater waking symptomatology was associated with less connectivity between fear-related seeds and anterior emotion regulatory regions, while greater SWS% was associated with more connectivity between these regions. Post-traumatic symptoms, including prolonged SOL, may reflect excessive activity in the salience network and lesser top-down control of this network by the prefrontal cortex. Larger samples will be needed to further characterize correlates of rsFC in this population.

Supplementary Material

Refer to Web version on PubMed Central for supplementary material.

Acknowledgments

The authors would like to thank Karen Gannon, RPSGT for scoring sleep recordings and Cherrysse Ulsa and Sabrina Fleishaker for assistance with data reduction.

Research was carried out at the Athinoula A. Martinos Center for Biomedical Imaging, Charlestown MA and the Massachusetts General Hospital, Department of Psychiatry, Psychiatric Neuroimaging Division.

Financial disclosures

This project was supported by NIMH grant R01MH109638 to E.P.S. The authors report no biomedical financial interests or potential conflicts of interest.

References

1. Germain A (2013): Sleep disturbances as the hallmark of PTSD: where are we now? Am J Psychiatry. 170:372–382. [PubMed: 23223954]

2. Pigeon WR, Mellman TA (2017): Dreams and nightmares in posttraumatic stress disorder In: Kryger MH, Roth T, Dement WC, editors. Principles and Practice of Sleep Medicine, Sixth Edition Philadelphia: Elsevier, pp 561–566.
3. Pace-Schott EF, Bottary RM (2018): Characterization, Conceptualization, and Treatment of Sleep Disturbances in PTSD In: Stoddard FJJ, Benedek DM, Milad MR, Ursano RJ, editors. Primer on Trauma- and Stressor-Related Disorders. Oxford University Press.
4. Marcks BA, Weisberg RB, Edelen MO, Keller MB (2010): The relationship between sleep disturbance and the course of anxiety disorders in primary care patients. Psychiatry Res. 178:487–492. [PubMed: 20537716]
5. Connelly M, Denney DR (2007): Regulation of emotions during experimental stress in alexithymia. J Psychosom Res. 62:649–656. [PubMed: 17540222]
6. Bardeen JR, Orcutt HK (2011): Attentional control as a moderator of the relationship between posttraumatic stress symptoms and attentional threat bias. J Anxiety Disord. 25:1008–1018. [PubMed: 21782385]
7. Cisler JM, Wolitzky-Taylor KB, Adams TG Jr., Babson KA, Badour CL, Willems JL (2011): The emotional Stroop task and posttraumatic stress disorder: a meta-analysis. Clin Psychol Rev. 31:817–828. [PubMed: 21545780]
8. Milad MR, Pitman RK, Ellis CB, Gold AL, Shin LM, Lasko NB, et al. (2009): Neurobiological basis of failure to recall extinction memory in posttraumatic stress disorder. Biol Psychiatry. 66:1075–1082. [PubMed: 19748076]
9. Fonzo GA, Simmons AN, Thorp SR, Norman SB, Paulus MP, Stein MB (2010): Exaggerated and disconnected insular-amygdalar blood oxygenation level-dependent response to threat-related emotional faces in women with intimate-partner violence posttraumatic stress disorder. Biol Psychiatry. 68:433–441. [PubMed: 20573339]
10. Shvil E, Rusch HL, Sullivan GM, Neria Y (2013): Neural, psychophysiological, and behavioral markers of fear processing in PTSD: a review of the literature. Curr Psychiatry Rep. 15:358. [PubMed: 23619614]
11. Morey RA, Dunsmoor JE, Haswell CC, Brown VM, Vora A, Weiner J, et al. (2015): Fear learning circuitry is biased toward generalization of fear associations in posttraumatic stress disorder. Transl Psychiatry. 5:e700. [PubMed: 26670285]
12. Lopresto D, Schipper P, Homberg JR (2016): Neural circuits and mechanisms involved in fear generalization: Implications for the pathophysiology and treatment of posttraumatic stress disorder. Neurosci Biobehav Rev. 60:31–42. [PubMed: 26519776]
13. Lazarov A, Suarez-Jimenez B, Tamman A, Falzon L, Zhu X, Edmondson DE, et al. (2019): Attention to threat in posttraumatic stress disorder as indexed by eye-tracking indices: a systematic review. Psychol Med. 49:705–726. [PubMed: 30178728]
14. Milad MR, Quirk GJ (2012): Fear extinction as a model for translational neuroscience: ten years of progress. Annual review of psychology. 63:129–151.
15. Shin LM, Liberzon I (2010): The neurocircuitry of fear, stress, and anxiety disorders. Neuropsychopharmacology. 35:169–191. [PubMed: 19625997]
16. Pace-Schott EF, Germain A, Milad MR (2015): Sleep and REM sleep disturbance in the pathophysiology of PTSD: the role of extinction memory. Biol Mood Anxiety Disord. 5:3. [PubMed: 26034578]
17. Rasch B, Born J (2013): About sleep's role in memory. Physiol Rev. 93:681–766. [PubMed: 23589831]
18. Goldstein AN, Walker MP (2014): The role of sleep in emotional brain function. Annu Rev Clin Psychol. 10:679–708. [PubMed: 24499013]
19. Pace-Schott EF, Germain A, Milad MR (2015): Effects of sleep on memory for conditioned fear and fear extinction. Psychol Bull. 141:835–857. [PubMed: 25894546]
20. Insel T, Cuthbert B, Garvey M, Heinssen R, Pine DS, Quinn K, et al. (2010): Research domain criteria (RDoC): toward a new classification framework for research on mental disorders. Am J Psychiatry. 167:748–751. [PubMed: 20595427]

21. Etkin A, Wager TD (2007): Functional neuroimaging of anxiety: a meta-analysis of emotional processing in PTSD, social anxiety disorder, and specific phobia. Am J Psychiatry. 164:1476–1488. [PubMed: 17898336]
22. Greicius MD, Supekar K, Menon V, Dougherty RF (2009): Resting-state functional connectivity reflects structural connectivity in the default mode network. Cereb Cortex. 19:72–78. [PubMed: 18403396]
23. Hagmann P, Cammoun L, Gigandet X, Meuli R, Honey CJ, Wedeen VJ, et al. (2008): Mapping the structural core of human cerebral cortex. PLoS Biol. 6:e159. [PubMed: 18597554]
24. van den Heuvel MP, Mandl RC, Kahn RS, Hulshoff Pol HE (2009): Functionally linked resting-state networks reflect the underlying structural connectivity architecture of the human brain. Hum Brain Mapp. 30:3127–3141. [PubMed: 19235882]
25. Vincent JL, Patel GH, Fox MD, Snyder AZ, Baker JT, Van Essen DC, et al. (2007): Intrinsic functional architecture in the anaesthetized monkey brain. Nature. 447:83–86. [PubMed: 17476267]
26. Fox MD, Raichle ME (2007): Spontaneous fluctuations in brain activity observed with functional magnetic resonance imaging. Nature reviews. 8:700–711.
27. Fox MD, Zhang D, Snyder AZ, Raichle ME (2009): The global signal and observed anticorrelated resting state brain networks. J Neurophysiol. 101:3270–3283. [PubMed: 19339462]
28. Raichle ME (2011): The restless brain. Brain connectivity. 1:3–12. [PubMed: 22432951]
29. Peterson A, Thome J, Frewen P, Lanius RA (2014): Resting-state neuroimaging studies: a new way of identifying differences and similarities among the anxiety disorders? Can J Psychiatry. 59:294–300. [PubMed: 25007403]
30. Seeley WW, Menon V, Schatzberg AF, Keller J, Glover GH, Kenna H, et al. (2007): Dissociable intrinsic connectivity networks for salience processing and executive control. J Neurosci. 27:2349–2356. [PubMed: 17329432]
31. Yeo BT, Krienen FM, Sepulcre J, Sabuncu MR, Lashkari D, Hollinshead M, et al. (2011): The organization of the human cerebral cortex estimated by intrinsic functional connectivity. J Neurophysiol. 106:1125–1165. [PubMed: 21653723]
32. Nicholson AA, Sapru I, Densmore M, Frewen PA, Neufeld RW, Theberge J, et al. (2016): Unique insula subregion resting-state functional connectivity with amygdala complexes in posttraumatic stress disorder and its dissociative subtype. Psychiatry Res Neuroimaging. 250:61–72. [PubMed: 27042977]
33. Olson EA, Kaiser RH, Pizzagalli DA, Rauch SL, Rosso IM (2018): Regional Prefrontal Resting-State Functional Connectivity in Posttraumatic Stress Disorder. Biol Psychiatry Cogn Neurosci Neuroimaging.
34. King AP, Block SR, Sripada RK, Rauch S, Giardino N, Favorite T, et al. (2016): Altered Default Mode Network (Dmn) Resting State Functional Connectivity Following a Mindfulness-Based Exposure Therapy for Posttraumatic Stress Disorder (Ptsd) in Combat Veterans of Afghanistan and Iraq. Depress Anxiety. 33:289–299. [PubMed: 27038410]
35. Koch SB, van Zuiden M, Nawijn L, Frijling JL, Veltman DJ, Olff M (2016): Aberrant Resting-State Brain Activity in Posttraumatic Stress Disorder: A Meta-Analysis and Systematic Review. Depress Anxiety. 33:592–605. [PubMed: 26918313]
36. Cuthbert BN (2014): The RDoC framework: facilitating transition from ICD/DSM to dimensional approaches that integrate neuroscience and psychopathology. World psychiatry : official journal of the World Psychiatric Association. 13:28–35.
37. Simpson HB (2012): The RDoC project: a new paradigm for investigating the pathophysiology of anxiety. Depression and anxiety. 29:251–252. [PubMed: 22511360]
38. Disner SG, Marquardt CA, Mueller BA, Burton PC, Sponheim SR (2018): Spontaneous neural activity differences in posttraumatic stress disorder: A quantitative resting-state meta-analysis and fMRI validation. Hum Brain Mapp. 39:837–850. [PubMed: 29143411]
39. Wang T, Liu J, Zhang J, Zhan W, Li L, Wu M, et al. (2016): Altered resting-state functional activity in posttraumatic stress disorder: A quantitative meta-analysis. Sci Rep. 6:27131. [PubMed: 27251865]

40. Rougemont-Bucking A, Linnman C, Zeffiro TA, Zeidan MA, Lebron-Milad K, Rodriguez-Romaguera J, et al. (2011): Altered processing of contextual information during fear extinction in PTSD: an fMRI study. CNS neuroscience & therapeutics. 17:227–236. [PubMed: 20406268]
41. Milad MR, Rauch SL (2012): Obsessive-compulsive disorder: beyond segregated cortico-striatal pathways. Trends Cogn Sci. 16:43–51. [PubMed: 22138231]
42. Ochsner KN, Gross JJ (2005): The cognitive control of emotion. Trends Cogn Sci. 9:242–249. [PubMed: 15866151]
43. Delgado MR, Nearing KI, Ledoux JE, Phelps EA (2008): Neural circuitry underlying the regulation of conditioned fear and its relation to extinction. Neuron. 59:829–838. [PubMed: 18786365]
44. First MB, Gibbon M, Spitzer RL, Williams JBW (2007): Structured Clinical Interview for DSM-IV-TR Axis I Disorders–Non-Patient Edition (SCIDI/NP). New York, NY: Biometrics Research Department, New York State Psychiatric Institute
45. Blake DD, Weathers FW, Nagy LM, Kaloupek DG, Gusman FD, Charney DS, et al. (1995): The development of a Clinician-Administered PTSD Scale. J Trauma Stress. 8:75–90. [PubMed: 7712061]
46. Blevins CA, Weathers FW, Davis MT, Witte TK, Domino JL (2015): The Posttraumatic Stress Disorder Checklist for DSM-5 (PCL-5): Development and Initial Psychometric Evaluation. J Trauma Stress. 28:489–498. [PubMed: 26606250]
47. Kushida CA, Chang A, Gadkary C, Guilleminault C, Carrillo O, Dement WC (2001): Comparison of actigraphic, polysomnographic, and subjective assessment of sleep parameters in sleep-disordered patients. Sleep Med. 2:389–396. [PubMed: 14592388]
48. Lichstein KL, Stone KC, Donaldson J, Nau SD, Soeffing JP, Murray D, et al. (2006): Actigraphy validation with insomnia. Sleep. 29:232–239. [PubMed: 16494091]
49. Pace-Schott EF, Kaji J, Stickgold R, Hobson JA (1994): Nightcap measurement of sleep quality in self-described good and poor sleepers. Sleep. 17:688–692. [PubMed: 7701179]
50. Pace-Schott EF, Stickgold R, Muzur A, Wigren PE, Ward AS, Hart CL, et al. (2005): Sleep quality deteriorates over a binge--abstinence cycle in chronic smoked cocaine users. Psychopharmacology (Berl). 179:873–883. [PubMed: 15672273]
51. Whitfield-Gabrieli S, Nieto-Castanon A (2012): Conn: a functional connectivity toolbox for correlated and anticorrelated brain networks. Brain Connect. 2:125–141. [PubMed: 22642651]
52. Behzadi Y, Restom K, Liau J, Liu TT (2007): A component based noise correction method (CompCor) for BOLD and perfusion based fMRI. Neuroimage. 37:90–101. [PubMed: 17560126]
53. Graham BM, Milad MR (2011): The study of fear extinction: implications for anxiety disorders. Am J Psychiatry. 168:1255–1265. [PubMed: 21865528]
54. Tzourio-Mazoyer N, Landeau B, Papathanassiou D, Crivello F, Etard O, Delcroix N, et al. (2002): Automated anatomical labeling of activations in SPM using a macroscopic anatomical parcellation of the MNI MRI single-subject brain. Neuroimage. 15:273–289. [PubMed: 11771995]
55. Maldjian JA, Laurienti PJ, Kraft RA, Burdette JH (2003): An automated method for neuroanatomic and cytoarchitectonic atlas-based interrogation of fMRI data sets. Neuroimage. 19:1233–1239. [PubMed: 12880848]
56. Yarkoni T, Poldrack RA, Nichols TE, Van Essen DC, Wager TD (2011): Large-scale automated synthesis of human functional neuroimaging data. Nat Methods. 8:665–670. [PubMed: 21706013]
57. Pace-Schott EF, Zimmerman JP, Bottary RM, Lee EG, Milad MR, Camprodon JA (2017): Resting state functional connectivity in primary insomnia, generalized anxiety disorder and controls. Psychiatry Res Neuroimaging. 265:26–34. [PubMed: 28500965]
58. Whitfield-Gabrieli S, Moran JM, Nieto-Castanon A, Triantafyllou C, Saxe R, Gabrieli JD (2011): Associations and dissociations between default and self-reference networks in the human brain. Neuroimage. 55:225–232. [PubMed: 21111832]
59. Winkler AM, Ridgway GR, Webster MA, Smith SM, Nichols TE (2014): Permutation inference for the general linear model. Neuroimage. 92:381–397. [PubMed: 24530839]
60. Eklund A, Nichols TE, Knutsson H (2016): Cluster failure: Why fMRI inferences for spatial extent have inflated false-positive rates. Proc Natl Acad Sci U S A. 113:7900–7905. [PubMed: 27357684]

61. Kobayashi I, Boarts JM, Delahanty DL (2007): Polysomnographically measured sleep abnormalities in PTSD: a meta-analytic review. Psychophysiology. 44:660–669. [PubMed: 17521374]

62. Mellman TA, Bustamante V, Fins AI, Pigeon WR, Nolan B (2002): REM sleep and the early development of posttraumatic stress disorder. Am J Psychiatry. 159:1696–1701. [PubMed: 12359675]

63. Cairney SA, Durrant SJ, Power R, Lewis PA (2015): Complementary roles of slow-wave sleep and rapid eye movement sleep in emotional memory consolidation. Cereb Cortex. 25:1565–1575. [PubMed: 24408956]

64. Hauner KK, Howard JD, Zelano C, Gottfried JA (2013): Stimulus-specific enhancement of fear extinction during slow wave sleep. Nat Neurosci.

65. Dodhia S, Hosanagar A, Fitzgerald DA, Labuschagne I, Wood AG, Nathan PJ, et al. (2014): Modulation of resting-state amygdala-frontal functional connectivity by oxytocin in generalized social anxiety disorder. Neuropsychopharmacology. 39:2061–2069. [PubMed: 24594871]

66. Pizzagalli DA (2011): Frontocingulate dysfunction in depression: toward biomarkers of treatment response. Neuropsychopharmacology. 36:183–206. [PubMed: 20861828]

67. Phelps EA, Delgado MR, Nearing KI, LeDoux JE (2004): Extinction learning in humans: role of the amygdala and vmPFC. Neuron. 43:897–905. [PubMed: 15363399]

68. LeDoux JE (2000): Emotion circuits in the brain. Annual review of neuroscience. 23:155–184.

69. Nachev P, Kennard C, Husain M (2008): Functional role of the supplementary and pre-supplementary motor areas. Nat Rev Neurosci. 9:856–869. [PubMed: 18843271]

70. Ridderinkhof KR, Ullsperger M, Crone EA, Nieuwenhuis S (2004): The role of the medial frontal cortex in cognitive control. Science. 306:443–447. [PubMed: 15486290]

71. Bonnelle V, Ham TE, Leech R, Kinnunen KM, Mehta MA, Greenwood RJ, et al. (2012): Salience network integrity predicts default mode network function after traumatic brain injury. Proc Natl Acad Sci U S A. 109:4690–4695. [PubMed: 22393019]

72. Olson IR, Plotzker A, Ezzyat Y (2007): The Enigmatic temporal pole: a review of findings on social and emotional processing. Brain. 130:1718–1731. [PubMed: 17392317]

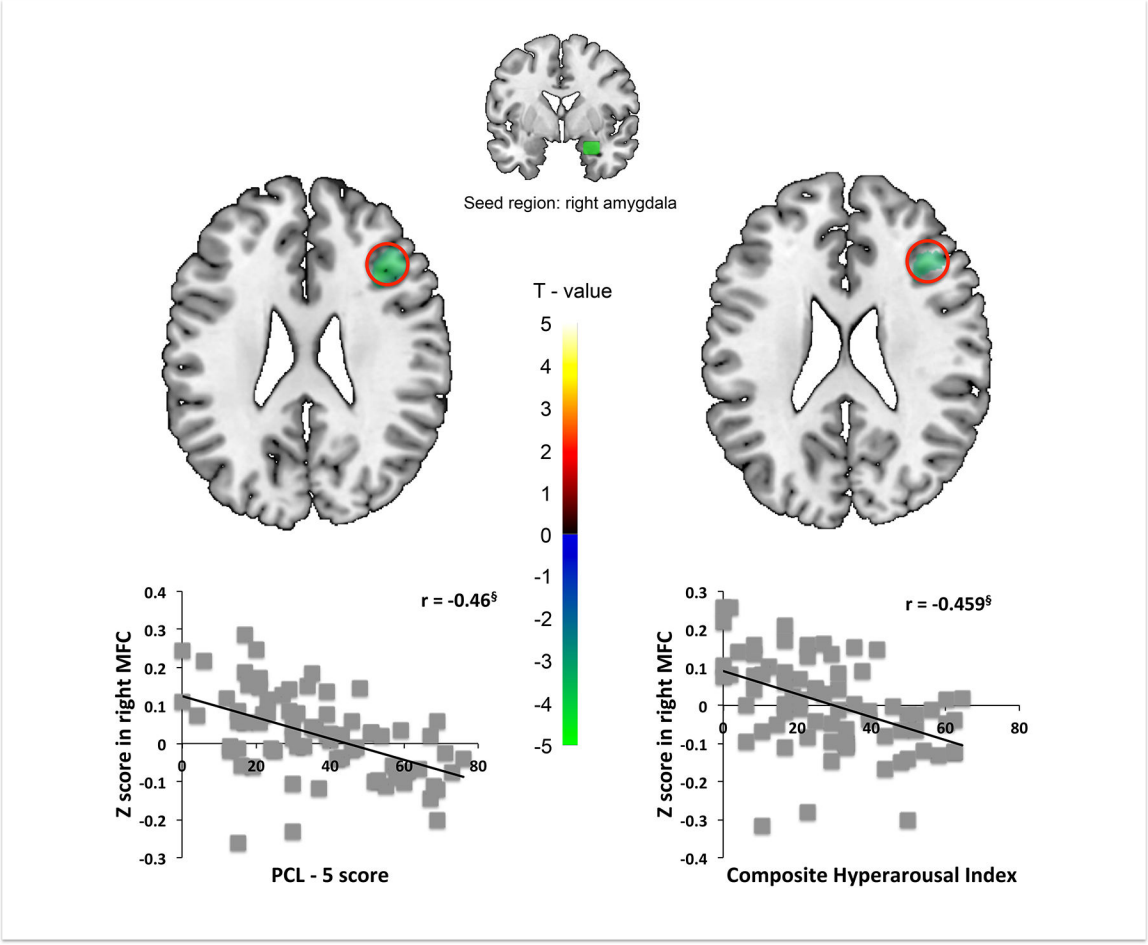

Figure 1.

PTSD severity (PCL-5; *left panel*) and composite hyperarousal index (CHI; *right panel*) predict lesser rsFC between right amygdala seed and right middle frontal cortex (MFC). PCL-5 *(left)* and CHI *(right)* correlate negatively with extracted amygdala-MFC mean Z-values. § $p < 0.001$

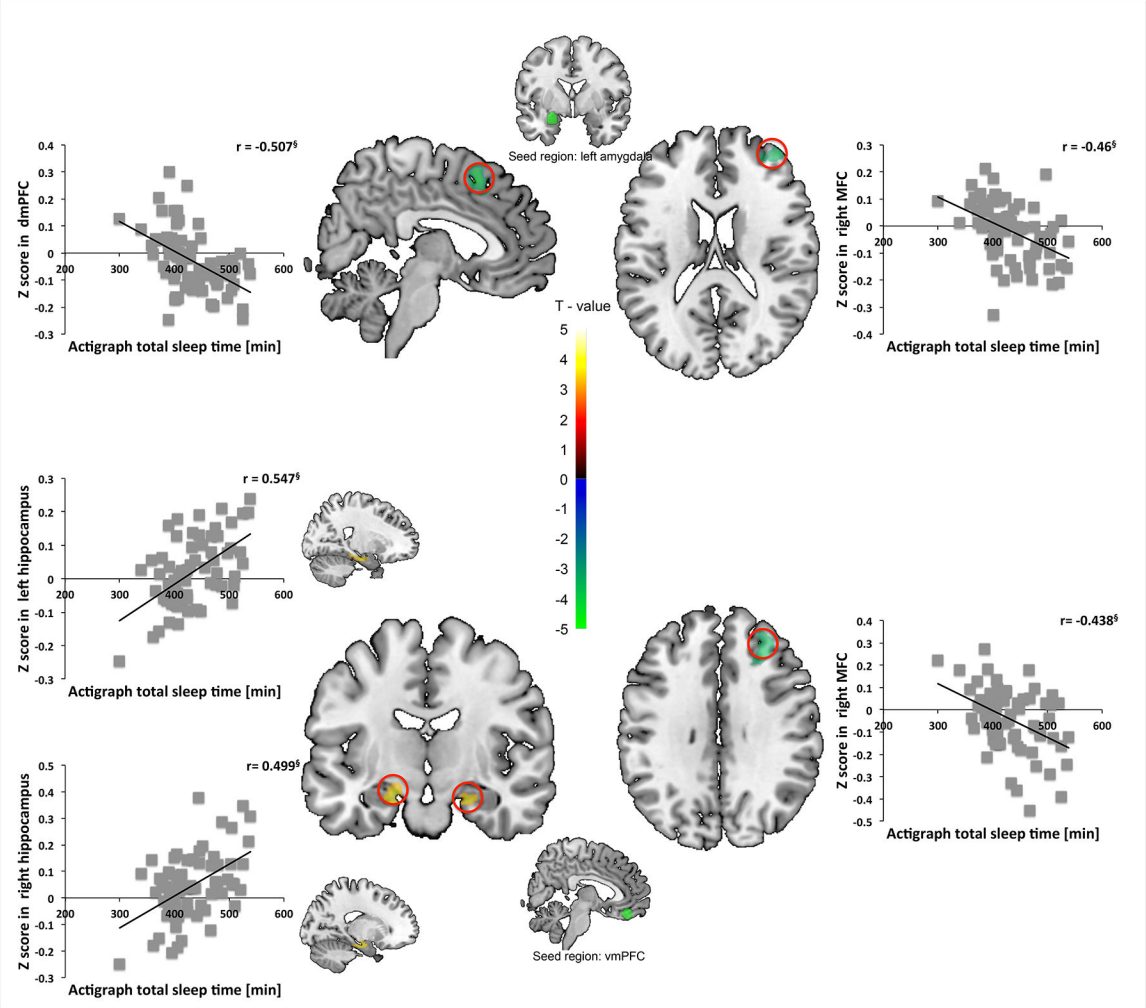

Figure 2.

Actigraph total sleep time (TST) predicts lesser rsFC between the left amygdala seed and the dorsomedial prefrontal cortex (dmPFC) and correlates negatively with extracted amygdala-dmPFC mean Z-values (*upper left panel*). TST predicts lesser rsFC between the left amygdala seed and the right middle frontal cortex (MFC) and correlates negatively with extracted amygdala-MFC mean Z-values *(upper right panel)*. TST predicts greater rsFC between vmPFC seed and bilateral hippocampi and correlates positively with extracted vmPFC-hippocampal mean Z-values *(lower left panel)*. TST predicts lesser rsFC between vmPFC seed and right MFC and correlates negatively with extracted vmPFCMFC mean Z-values *(lower right panel)*. § $p < 0.001$

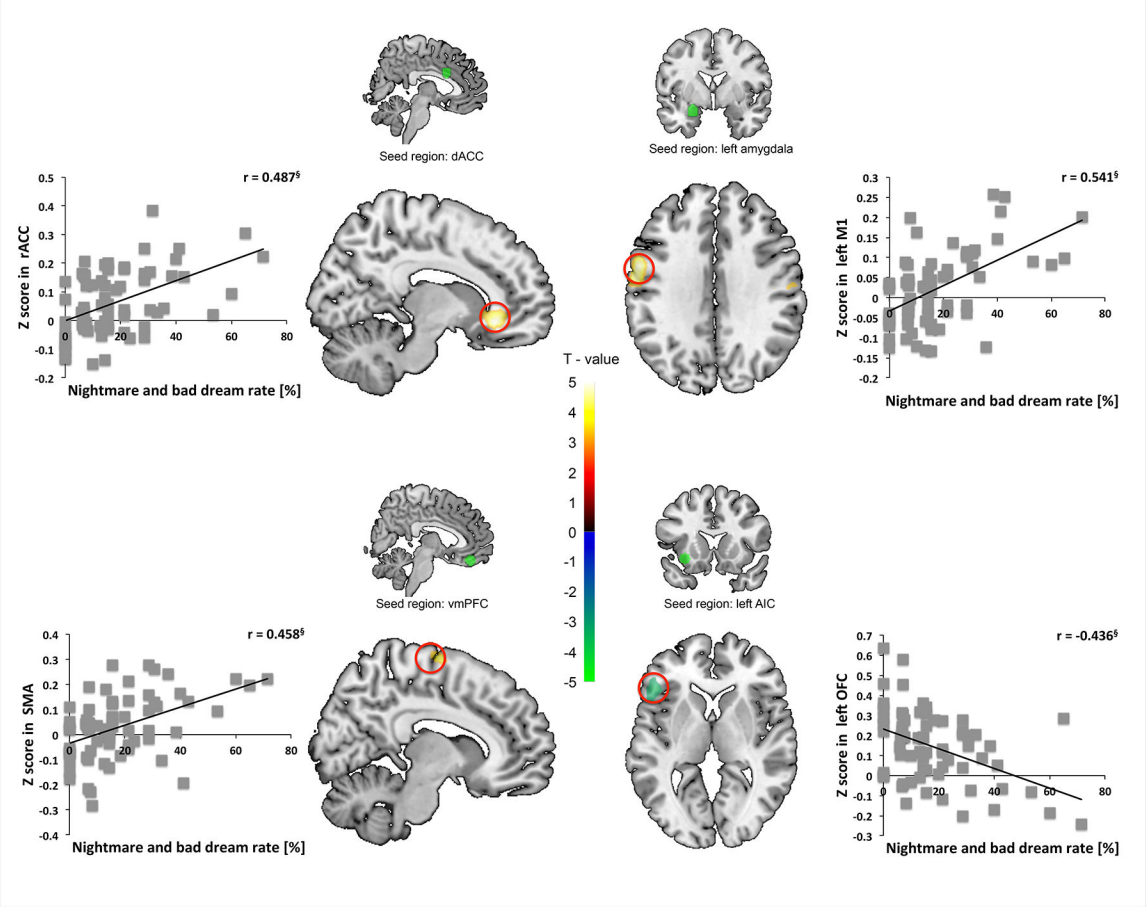

Figure 3.

Nightmare-plus-bad-dream rate (Nightmares) predicts greater rsFC between the dACC seed and the rostral ACC (rACC) and correlates positively with extracted dACC-rACC mean Z-values *(upper left panel)*. Nightmares predict greater rsFC between the left amygdala seed and the left primary motor cortex (M1) and correlate positively with extracted amygdala-M1 mean Z-values *(upper right panel)*. Nightmares predict more rsFC between the vmPFC seed and the supplementary motor cortex (SMA) and correlate positively with extracted vmPFC-SMA mean Z-values *(lower left panel)*. Nightmares predict lesser rsFC between left AIC seed and the left orbitofrontal cortex (OFC) and correlate positively with extracted AIC-OFC mean Z-values *(lower right panel)*. § $p < 0.001$

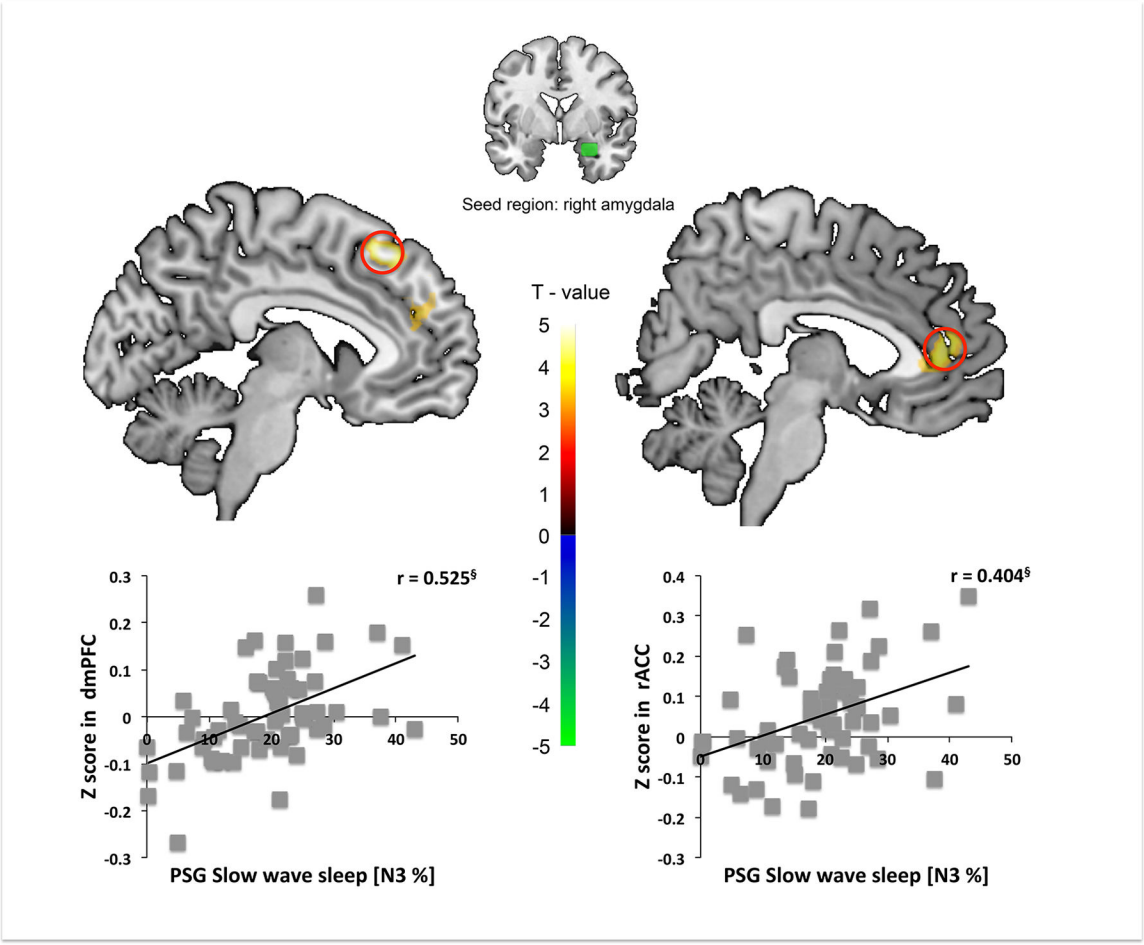

Figure 4.

Percent slow wave sleep (SWS%) predicts lesser rsFC between the right amygdala seed and the dorsomedial PFC (dmPFC) and correlates positively with extracted amygdala-dmPFC mean Z-values *(left panel)*. SWS% predicts greater rsFC between the right amygdala seed and the rostral ACC (rACC) and correlates positively with extracted amygdala-rACC mean Z-values *(right panel)*. § $p < 0.001$

Table 1.

Group means, standard deviations and ranges of demographic and sleep characteristics among total sample of trauma-exposed individuals (N=74).

	Mean ± SD	Minimum value	Maximum value
Demographics			
Number of subjects	74		
Number of males	25		
Age (years)	23.5±4.5	18	40
Educational level			
High school or equivalent	5		
Some college	27		
Bachelor's (or Associates) Degree	24		
Graduate Degree	11		
Unknown or not reported	7		
PTSD symptom			
CAPS total score	27.4±16.6	0	58
PCL-5 total score	36.6±19.7	0	76
PSI (0–100 scale) *†	31.3±16.4	0	61.9
CHI (0–100 scale) *†	28.8±18.3	0	64.6
Time since trauma (months)	12.3±6.9	1	28
Sleep questionnaires			
PSQI	7.13±3.3	2	14
ESS	7.13±4.7	0	19
MEQ	46.43±9.6	25	68
Actigraph data			
Total sleep time (min) *	432.4±51.5	299.7	538.9
Sleep efficiency (%) *	90.7±4.7	77.9	97.8
Sleep onset latency (min) *	23.2±18.8	2	86.2
Sleep midpoint (min after 24:00) #	290.3±82.4	167.2	609
Sleep diary data			
Total sleep time (min) *	432.5±59.8	249.5	570.9
Sleep efficiency (%) *	92.0±6.1	66.5	99.2
Sleep onset latency (min) *	22.5±14.6	3	69.2
Number of dreams	6.2±3.8	0	15
Number nightmares & bad dreams	2.7±2.8	0	13
nightmares and bad dreams rate (%)	48.4±30.2	0	100
PSG data			
Total sleep time (min)	374.2±124.5	48.5	635
N1 %	6.5±3.9	0.9	17.6
N2 %	53.8±9.9	21.8	70.5

	Mean ± SD	Minimum value	Maximum value
Sleep onset latency	26.5±39.1	0	255
REM latency	94.7±48.1	0	243.5
Slow wave sleep (%) *	21.6±12.5	0.3	62.3
REM (%) *	18.1±6.9	0	42.1
Sleep efficiency (%)	85.2±11.9	29.5	98.0

Abbreviations: CAPS – Clinician-Administered PTSD Scale; PCL-5 – PTSD Checklist-5; PSI – PTSD symptom severity; CHI – composite hyperarousal index; PSQI–Pittsburgh Sleep Quality Index; ESS – Epworth Sleepiness Scale; MEQ – Morningness-Eveningness Questionnaire; NEO PI-R – NEO Personality Inventory-Revised; PSG – polysomnography.

*Predictor values selected *pre-hoc* for rsFC analyses

†PSI was calculated using the CAPS and PCL-5 excluding hyperarousal questions and CHI was calculated from the hyperarousal questions from the CAPS and PCL-5. For both indices, respective partial CAPS and PCL-5 raw scores were first converted to a 0–100 scale and then the 2 resulting values were averaged.

#Sleep midpoint was computed as the midpoint between sleep onset and final awakening (expressed as minutes past midnight).

Biol Psychiatry Cogn Neurosci Neuroimaging. Author manuscript; available in PMC 2020 December 01.

Table 2.

Correlation of posttraumatic symptom, sleep quality and sleep architecture variables with resting state connectivity of 5 fear-related and 1 emotion regulatory seed regions with anterior cerebral voxel clusters surviving family-wise error (FWE) correction using statistical non-parametric mapping (SnPM).

Predictor	Direction	Seed	Connected regions with seed	x, y, z (peak voxel)	peak t	k	Threshold k with SnPM
Symptom							
PCL-5	Negative	right amygdala	right middle frontal cortex (BA9)	40,26,24	4.33	365	204**
CHI	Negative	right amygdala	right middle frontal cortex (BA9)	40,26,26	3.73	170	122*
Actigraphy							
Actigraph TST	Negative	left amygdala	dmPFC (SMA; BA8, 32, 6)	2,18,54	4.49	417	182**
	Negative	vmPFC	right middle frontal cortex (BA9, 10)	30,34,36	4.03	288	197**
	Positive	vmPFC	left hippocampus	−20,−12,−20	4.02	313	183**
	Negative	left amygdala	right middle frontal cortex (BA10)	38,50,20	3.73	173	113*
	Positive	vmPFC	right hippocampus	24,−12,−20	3.85	161	126*
Actigraph SOL	Positive	dACC	right posterior insular cortex (BA13)	42,−10,0	4.4	292	205**
	Positive	left amygdala	left insular cortex (BA13)	−40,6,−8	4.14	324	228**
	Positive	vmPFC	right primary motor cortex (BA4)	28,−24,64	4.26	326	200**
	Positive	left AIC	right middle frontal cortex (BA10)	30,52,14	3.76	233	206**
	Positive	dACC	left posterior insular cortex (BA13)	−40,−16,2	3.67	153	134*
	Positive	left amygdala	right insular cortex (BA13)	42,8,−14	4.13	169	140*
Actigraph SE	Negative	vmPFC	SMA (BA6)	2,−16,72	4.52	636	184**
Diary							
Diary TST	Negative	left AIC	subgenual ACC (BA25)	6,12,−12	3.87	135	131*
	Positive	dACC	rACC (BA24)	0,30,18	3.95	162	120*
Diary SOL	Positive	right AIC	pre-SMA (BA8, 6, 9)	−2,42,52	4.48	492	203**
	Positive	right AIC	left temporal pole (BA38, 21)	−42,18,−26	3.84	276	203**
Nightmare and Bad dream rate	Positive	dACC	rACC (BA24)	10,32,−8	4.89	309	188**
	Positive	left amygdala	left primary motor cortex (BA6, 4, 9)	−56,0,30	4.97	305	205**
	Negative	left AIC	left orbitofrontal cortex (BA47)	−48,28,4	3.81	157	123*
	Positive	vmPFC	SMA (BA6)	8,−8,70	3.87	133	132*
PSG							

Predictor	Direction	Seed	Connected regions with seed	x, y, z (peak voxel)	peak t	k	Threshold k with SnPM
SWS%	Positive	right amygdala	dmPFC (BA8, 9)	−6,28,50	5.21	643	198**
	Positive	right amygdala	rACC (BA32)	8,44,8	4.14	218	198**

Abbreviations: PCL-5 – PTSD Checklist for DSM-5; CHI – composite hyperarousal index; BA – brodmann area; TST – total sleep time; dmPFC – dorsomedial prefrontal cortex; SMA – supplementary motor areas; vmPFC – ventromedial prefrontal cortex; SOL – sleep onset latency; dACC – dorsal anterior cingulate cortex; AIC – anterior insular cortex; SE – sleep efficiency; rACC – rostral anterior cingulate cortex; PSG – polysomnography; SWS – slow wave sleep. k – the number of contiguous voxels in a cluster whose mean connectivity with the respective seed showed significant correlation with the respective sleep or symptom predictor variable using SPM. Threshold k with SnPM – minimum number of contiguous voxels in a cluster that the SnPM correction determined sufficiently large to not be a false positive at p<0.1* or p<0.05**.

Biol Psychiatry Cogn Neurosci Neuroimaging. Author manuscript; available in PMC 2020 December 01.